

Development of Casein Microgels from Cross-Linking of Casein Micelles by Genipin

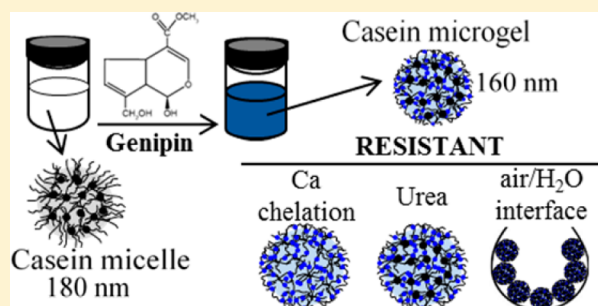
Naaman F. Nogueira Silva,^{*,†} Arnaud Saint-Jalmes,[‡] Antônio F. de Carvalho,[§] and Frédéric Gaucheron^{*,†}

[†]Agrocampus Ouest, UMR Science et Technologie du Lait et de l'Œuf, INRA, 35042 Rennes, France

[‡]Institut de Physique de Rennes, UMR CNRS, Université de Rennes, 35000 Rennes, France

[§]Departamento de Tecnologia de Alimentos, Universidade Federal de Viçosa, 36570-000 Viçosa, Brazil

ABSTRACT: Casein micelles are porous colloidal particles, constituted of casein molecules, water, and minerals. The vulnerability of the supramolecular structure of casein micelles face to changes in the environmental conditions restrains their applications in other domains besides food. Thus, redesigning casein micelles is a challenge to create new functionalities for these biosourced particles. The objective of this work was to create stable casein microgels from casein micelles using a natural cross-linker, named genipin. Suspensions of purified casein micelles (25 g L^{-1}) were mixed with genipin solutions to have final concentrations of 5, 10, and 20 mM genipin. Covalently linked casein microgels were formed via cross-linking of lysyl and arginyl residues of casein molecules. The reacted products exhibited blue color. The cross-linking reaction induced gradual changes on the colloidal properties of the particles. The casein microgels were smaller and more negatively charged and presented smoother surfaces than casein micelles. These results were explained based on the cross-linking of free NH_2 present in an external layer of κ -casein. Light scattering and rheological measurements showed that the reaction between genipin and casein molecules was intramicellar, as one single population of particles was observed and the values of viscosity (and, consequently, the volume fraction of the particles) were reduced. Contrary to the casein micelles, the casein microgels were resistant to the presence of dissociating agents, e.g., citrate (calcium chelating) and urea, but swelled as a consequence of internal electrostatic repulsion and the disruption of hydrophobic interactions between protein chains. The casein microgels did not dissociate at the air–solution interface and formed solid-like interfaces rather than a viscoelastic gel. The potential use of casein microgels as adaptable nanocarriers is proposed in the article.



INTRODUCTION

Casein micelles (CMs), the main colloidal particles present in skimmed milk,¹ are essentially constituted of proteins, minerals, and water. The casein content (25 g L^{-1} of milk) comprises four caseins molecules, named α_{S1} - (40%), α_{S2} - (10%), β - (35%), and κ -caseins (15%).² These caseins are rheomorphic proteins³ that possess different amino acid sequences and exhibit additional heterogeneity due to two post-translational modifications. The α_{S1} -, α_{S2} -, and β -caseins undergo extensive phosphorylation on their serine residues and form the “phosphate centers” (SerP-SerP-SerP-X-SerP), and κ -casein is glycosylated.² The CMs contain 7% of inorganic matter in a dry basis, composed mainly by colloidal calcium phosphate (CCP).⁴ CCP exists as spherical nanoclusters of $\sim 2\text{--}3 \text{ nm}$, surrounded by phosphate centers of α_{S1} -, α_{S2} -, and β -caseins.⁵ The assemblies of phosphorylated caseins with a core of CCP are the building blocks of CMs, in which the casein tails of the assemblies interact by means of weak interactions, creating a three-dimensional mesh.⁶ This mesh is sterically stabilized by an external layer of κ -casein,^{1,6} which can be described as a “salted polyelectrolyte brush”.⁷ The CMs are porous supramolecular aggregates of about 200 nm .^{1,4} Assuming a Gaussian distribution, CMs exhibited a polydispersity of 0.38 with

diameters ranging from ~ 80 to 550 nm .³ The other major component of CMs is water. Indeed, they are highly hydrated, internally and externally ($\sim 4 \text{ g}$ of water per g of protein⁴), and possess water-filled cavities (~ 20 to 30 nm) and channels ($> 5 \text{ nm}$)⁸ within the micellar structure whereby salts, proteins, enzymes, and polymers pass through.¹

The integrity of CMs depends on the physicochemical conditions of the medium. On the one hand, CMs destabilize and coagulate when the external layer of κ -casein is enzymatically cleaved or collapsed by alcohol addition.⁹ On the other hand, CMs dissociate by urea addition,¹⁰ by alkalizing the medium above $\text{pH} \sim 8$,¹¹ and when CCP is solubilized by calcium chelating salts.^{12,13} Acidification, below $\text{pH} 5$, specifically induces coagulation and subsequent dissociation of CMs.¹⁴

Caseins, in general, have many applications in food¹⁴ and chemical industries,¹⁵ and their state of aggregation affects the properties of the products where they are used. Thus, the production of stable CMs can expand their spectra of

Received: November 15, 2013

Revised: August 11, 2014

application by reducing their sensitivity to the physicochemical environment. In this regard, it was shown that CMs can be enzymatically cross-linked by transglutaminase.^{16,17} Their internal structure was not affected when analyzed by small-angle X-ray scattering (SAXS) and small-angle neutron scattering (SANS).⁶ These cross-linked CMs swelled in the presence of dissociating agents as citrate or urea.¹⁶ The CMs so modified were referred as casein microgel particles.¹⁶

Recently, it was demonstrated that isolated caseins molecules react with a cross-linker named genipin (GP) and form a gel.¹⁸ GP is a natural molecule extracted from *Gardenia jasminoides*¹⁹ which reacts with free amino groups of proteins and generates blue pigments. *In vitro* studies showed that GP is 10⁴ less cytotoxic than glutaraldehyde,²⁰ which is a classical protein cross-linker.

The aims of our work were to produce stable casein microgels by using GP and CMs and study their new colloidal properties. The cross-linking reaction was followed by the development of blue pigments. Then, the samples were characterized with respect to the amino acids involved in the reaction and the formation of covalent products. Next, the particles were studied regarding their sizes, shapes, and charges. The consequence of the reaction on their volume fractions was calculated from viscosity and from hydrodynamic radius. Following this, their stabilities were verified against dissociating agents, adsorption at air/water interface, and cycles of interfacial compression and expansion.

MATERIALS AND METHODS

Materials. Powder of purified CMs (free of whey proteins) was obtained by microfiltration of raw skimmed milk (0.1 μm pore size), followed by diafiltration against Milli-Q water²¹ and spray-drying.²² In our study, a suspension of micellar casein was obtained by dispersing the powder of CMs at 27.5 g L⁻¹ of casein in a buffer solution containing 25 mM of 4-(2-hydroxyethyl)-1-piperazine ethanesulfonic acid (HEPES), 2 mM CaCl₂ at pH 7.10. Sodium azide at 0.25 g L⁻¹ (Sigma, Saint Louis, MO) was added to prevent microbial growth.

Genipin (GP) was purchased from Challenge Bioproducts Co. Ltd. (Yun-Lin Hsien, Taiwan, Republic of China) with a purity of 98%. GP was dissolved in a mixture of 74/26 (w/w) HEPES buffer and absolute ethanol to have a stock solution at 200 mM.

The CMs suspension and GP solution were mixed to have final concentrations of 5, 10, and 20 mM GP at a same final concentration of caseins (25 g L⁻¹). The dilutions caused by the addition of GP were corrected by adding HEPES buffer and/or absolute ethanol. Initially, the reaction was carried out at 50 °C for 24 h. Then, samples were kept at 4 °C for 26 h prior analyses. A control sample without GP was treated in the same conditions. The results represent the mean of three independent repetitions.

Visible Spectroscopy. The reaction between CMs and GP was followed as a function of time for 50 h by spectroscopy. Visible spectra between 550 and 650 nm were recorded at different times at 20 °C by using a spectrometer (Uvikon 922, Kontron, Milan, Italy). As a maximum of absorbance was verified at 607 nm (data not shown), this wavelength was selected to highlight the reaction.²³ The CMs suspensions were diluted 1/33 in HEPES buffer before measuring the absorbance.

Amino Acid Compositions. The amino acids involved in the reaction with GP were identified and quantified by analysis of the total amino acid composition of each suspension. These compositions were determined after hydrolysis of 70 mg of the different suspensions in sealed tubes in the presence of 1 mL of 6 N HCl for 24 h at 110 °C.²⁴ Hydrolyzates were evaporated to dryness in vacuum, washed twice with distilled water, and analyzed by cation-exchange chromatography with an automatic amino acid analyzer (Biochrom 30 AAA, Cambridge, UK) using lithium citrate buffer for elution.²⁵

Genipin Concentration. The efficiency of the reaction between CMs and GP was also evaluated by quantifying the free GP. Free GP concentration was determined by reverse-phase high performance liquid chromatography (RP-HPLC) (Dionex ICS 3000, Voisin le-Bretonneux, France) according to Sheu and Hsin (1998)²⁶ with modifications. The RP column was a Vydac C18 (218TP54, Touzart & Matignon, France). Separation was done using a linear gradient elution with eluent A (5 mM NaH₂PO₄ adjusted to pH 4.6) and eluent B (CH₃OH:CH₃CN:buffer A = 9:9:2) according to the following gradient: 0–22 min, 5–45% B; 22–32 min, 45–5% B. The flow rate was 0.8 mL min⁻¹, and free GP was detected at 240 nm. A calibration curve was established, and the GP was eluted between 15 and 16 min. The suspensions were previously filtered through a Vivaspine 20 concentrator (molecular weight cutoff = 10 kDa; Vivascience, Palaiseau, France). Then, the recovered filtrates containing free GP were diluted 1/100 in buffer A prior injection of 20 μL .

Chromatography of Casein Molecules. The modifications of casein molecules by GP were evaluated by RP-HPLC as described by Silva et al.²⁷ (Dionex ICS 3000, Voisin le-Bretonneux, France). A RP column of 15 cm Vydac C4 (214TP54, Touzart & Matignon, France) was used. Prior to injection, CMs were submitted to dissociation conditions in the presence of 7.5 M urea and 100 mM sodium citrate (pH 8.3) and then acidified by trifluoroacetic acid to pH ~2. Mixtures were filtered through a membrane (pore size of 0.45 μm) before injection of 50 μL , i.e., ~80 μg of caseins.

Hydrodynamic Diameter (D_h). The average D_h of CMs was measured by dynamic light scattering (DLS) on a Zetasizer Nano ZS (Malvern Instruments, Worcestershire, United Kingdom). Measurements were carried out at a scattering angle of 173° and a wavelength of 633 nm. The average D_h was calculated using the Stokes–Einstein relation and assuming that particles have a spherical shape. Suspensions were previously diluted 1/25 in 25 mM HEPES, 2 mM Ca at pH 7.10, filtered on a membrane with a pore size of 0.45 μm to eliminate possible dusty particles and left at 20 °C for 20 min. The viscosity of the solution was 1.003 mPa s⁻¹ at 20 °C.

DLS was also used to study the resistance of particles against dissociating agents (with same equipment and conditions than for those used for average D_h). The suspensions were diluted 1/25 in 100 mM sodium citrate at pH 7.10 or in 8 M urea at pH 9.30. The viscosities of these solutions were 1.033 and 1.686 mPa s⁻¹ at 20 °C, respectively.

Shape and Surface. Scanning electron microscopy (SEM) was used to appreciate the shape and surface aspects of CMs. Polyacrylamide membranes (Millipore SAS, Molsheim, France) with an average pore diameter of 0.22 μm were immersed into suspensions for 15 h. Then, CMs were fixed to the membrane by immersion in solution containing 2.0% (v/v) glutaraldehyde (Sigma-Aldrich, St. Louis, MO), 25 mM HEPES, and 2 mM CaCl₂ at pH 7.10 for 60 min. Next, membranes were rinsed in the same solution, without glutaraldehyde, and dehydrated using an ethanol gradient from 70% to absolute ethanol. Absolute ethanol was changed extensively to remove residual water. After that, membranes were dried to critical point CO₂ with a EM CPD300 drying system (Leica, Vienna, Austria), gold-coated in a JEOL JFC 1100 apparatus (JEOL, Tokyo, Japan), and observed in a JEOL JSM 6301F field emission microscope operated at 7 kV.

Zeta-Potential (ζ). ζ was determined in the same equipment and conditions than those previously described for D_h . Suspensions were diluted 1/25 in 25 mM HEPES, 2 mM Ca at pH 7.10 and left at 20 °C for 20 min before analysis. The applied voltage was set at 50 V. The dielectric constant (ϵ) and the refractive index were 80 and 1.333, respectively. Measurement of the negative charge of micelles was calculated from the electrophoretic mobility (U_E) and then applying the Henry equation, as follows:

$$U_E = 2\epsilon\zeta f(Ka)/3\eta$$

where ζ is the zeta potential, η the viscosity of the solvent and $f(Ka)$ the Henry's function (a value of 1.5 was used for $f(Ka)$, and in this case is referred to as the Smoluchowski approximation).

Volume Fraction (φ) of CMs from Viscosity and D_h . φ is a dimensionless quantity that expresses the ratio between the volume of a constituent i in a mixture and the total volume. First, the volume fraction φ of the CMs was calculated from the Krieger–Dougherty equation:

$$\eta = \eta_0 (1 - \varphi / \varphi_{\max})^{-2.5\varphi_{\max}}$$

where η_0 denotes the viscosity of the continuous phase and φ_{\max} the maximum volume fraction attainable. In our calculations, a value of 0.78 was used as φ_{\max} .²⁸ As the Krieger–Dougherty equation is an empirical formula, φ will be referred to as apparent φ . The measurements of viscosity were conducted at 20 °C with a Low-Shear 30 viscometer (Contraves, Zurich, Switzerland) using coaxial cylinders at shear rates ranging from 3 to 70 s⁻¹. The viscosity of the continuous phases was measured after filtering the suspensions through a Vivaspine 20 concentrator (molecular weight cutoff = 10 kDa; Vivascience, Palaiseau, France). The measured value of η_0 was 1.202 ± 0.002 mPa s⁻¹.

Second, φ was calculated from the average D_h (obtained from DLS), as follows:

$$\varphi = (NV_p) / V_{\text{total}}$$

where V_p is a volume of a single particle ($4/3\pi(D_h/2)^3$) and N is the number of particles, which was estimated as the mass of total caseins (g) divided by the mass of one particle. The average unitary mass of the CMs was taken from Glantz et al.,²⁹ who used asymmetrical flow field flow fractionation coupled with multiangle static light scattering to calculate the molecular weight of CMs. The average molecular weight of CMs was 4.4×10^8 g mol⁻¹. Then, we calculated the mass of one single micelle as being 7.3×10^{-16} g through the Avogadro constant.

Surface Tension (γ) and Interfacial Dilational Rheology. γ and interfacial dilational rheology were measured at 20 °C by using an oscillatory drop tensiometer (Tracker, Teclis, France). Drops of 10 μ L were formed at the tip of a syringe containing the suspensions. Image acquisition permitted the determination of the drop profile, which was used to calculate the surface tension. Under mechanical equilibrium of capillary and gravity forces, the Laplace equation relies pressure difference across the interface, γ , and the surface curvature.³⁰

When γ reached the equilibrium (i.e., plateau value of γ), the interfacial dilational moduli were determined by applying a sinusoidal oscillation of the volume drop at a frequency ν (typically, the amplitude of the volume variation is 10%, and the $\nu = 0.2$ Hz).³¹ Varying the volume corresponds to controlled oscillatory compression/dilation of the interfacial area A . The elastic and viscous moduli, E' and E'' , of the complex interfacial dilational modulus (E^*) are then obtained by monitoring the surface tension oscillation $\gamma(t)$. The oscillations of $A(t)$ and $\gamma(t)$ are not necessarily in phase: E' thus corresponds to a γ in phase with $A(t)$, while E'' corresponds to a response proportional to dA/dt and the phase shift ϕ (such as $\tan \phi = E''/E'$) varies from 0 to 90°. For purely elastic and solid-like interfacial layers, $E' \gg E''$ and ϕ tends to 0, whereas viscous and fluid-like interfacial layers have $E'' > E'$ and large ϕ .

In most of the works, performing such dilational viscoelasticity measurements and measuring E' and E'' is made to elucidate the dynamics of adsorption/desorption mechanisms of amphiphilic molecules (proteins, surfactants, or polymers) at a liquid interface, and this requires to investigate how the moduli depend on the oscillation frequency.³⁰ Here, the interfacial dilational rheology was used to provide information on the organization and stability of the particles once adsorbed at the hydrophobic air–solution interface, and this only requires measurements at a single low frequency.

RESULTS

The order of the results follows the same sequence described in the Methods section, i.e., from molecular level to particle and bulk scales. The results concerning CMs in control sample are

compared with those from the literature, since the physicochemical properties of CMs are already well-known.

Characterization of the Reaction between CMs and GP. The absorbance values as a function of reaction time for the different samples are presented in Figure 1. No change was

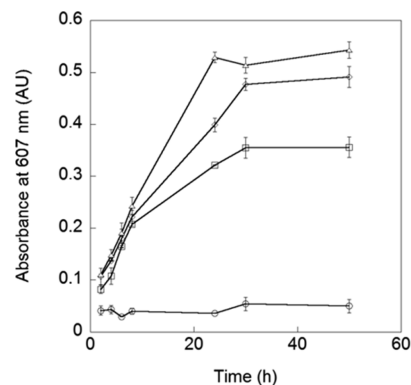


Figure 1. Arbitrary units (AU) of absorbance at 607 nm as a function time of control sample (○), 10 mM GP (◇), and 20 mM GP (△). Reaction was carried out at 50 °C for 24 h, and then the samples were kept at 4 °C for 26 h before their analyses.

observed for the control sample. With suspensions containing GP, the absorbance values increased as a function of time and GP concentration (20 > 10 > 5 mM), and the maximal values were reached after about 30 h of reaction (Figure 1).

The analyses of the total amino acid composition revealed that only lysyl and arginyl residues participated in the reaction between casein molecules and GP (Table 1). The concentrations of the others amino acids were constant for all samples (data not shown). However, lysyl and arginyl residues were consumed at different rates and as a function of the GP concentration (Table 1). Thus, when 20 mM GP was added, 14% of arginyl and 92% of lysyl residues were consumed.

The concentrations of the remaining GP are also reported in Table 1. GP reacted completely when 5 mM was added. Only a small fraction (0.3%) was determined after addition of 10 mM, and about 12% of GP did not reacted when it was added at a concentration of 20 mM.

Figure 2 shows the RP-HPLC profile of caseins molecules under dissociation conditions of CMs. For the control sample, a classical elution profile of caseins was obtained.³² The κ - and α_{S2} -caseins were eluted between 13 and 21 min. Their concomitant elution was due to different levels of glycosylation of κ -casein and phosphorylation of α_{S2} -casein.³² They were followed by a chromatographic peak of α_{S1} -casein at 22 min and then β -casein between 25 and 26 min. The two chromatographic peaks of β -caseins corresponded to the two major genetic variants.^{2,32} In the presence of 5 mM GP, only traces of the individual caseins were observed, and a new chromatographic peak was detected at the end of the elution (about 33 min). In the presence of 10 and 20 mM GP, individual caseins were not detected, and the intensity of the last chromatographic peak increased.

Particle-Scale Results. The average D_h (s) of CMs diluted in different solutions are shown in Table 2. The size distributions revealed one single population for all treatments (data not shown). The average D_h of CMs in control sample (diluted in HEPES buffer) was 179 nm, which was in close agreement with values reported for CMs.²⁹ When GP added

Table 1. Concentrations of Lysyl and Arginyl Residues and Remaining Free GP as a Function of the Initial GP Concentrations

	control	5 mM GP	10 mM GP	20 mM GP
free lysine (mM)	14.55 ± 0.35	10.84 ± 0.18	6.71 ± 0.02	1.08 ± 0.39
free arginine (mM)	5.56 ± 0.18	5.40 ± 0.11	5.05 ± 0.06	4.86 ± 0.04
total NH ₂ reacted	0	3.87	8.35	14.16
not reacted GP (mM)		^a	0.03 ± 0.01	2.34 ± 0.01

^aSymbols correspond to concentration lower than 0.001 mM.

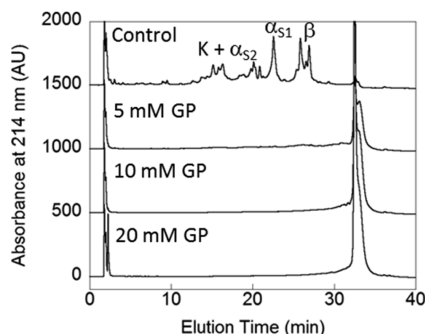


Figure 2. RP-HPLC profiles of casein molecules present in CMs suspensions containing 0 (control), 5, 10, and 20 mM GP. Before injection, CMs were dissociated by urea and citrate. The scale of absorbance values (in arbitrary units, AU) was changed for clarity.

samples were diluted in HEPES buffer, the averages D_h of CMs decreased compared to the control but were similar between them.

Using solutions of 100 mM sodium citrate or 8 M urea, the CMs were not detected in control sample (the DLS signal was noisy and autocorrelation functions could not be calculated). On the contrary, when the GP treated samples were diluted in these solutions, the average D_h (s) increased inversely to the GP concentration for all the solutions. The higher the GP concentrations were, the lower was the increase in size.

Figure 3 shows representative images of CMs obtained by SEM of the different suspensions. The diameters of CMs ranged from 100 to 300 nm in all samples. Classical images of CMs, presenting a roughly surface, were observed in the control sample.³³ However, the surfaces of CMs became gradually smooth when GP was used. It is noteworthy that no aggregated CMs were observed.

The zeta potential values ζ are presented in Table 2 for the different samples. The value of -18.4 mV found for the control sample was close to those reported in the literature.¹ The ζ values gradually decreased according to the GP addition.

Macroscopic Properties: Viscosity and Interfacial Results. All samples behaved as Newtonian fluids at the shear rates used ($3\text{--}70\text{ s}^{-1}$) and the viscosity decreased as a function of the GP addition (Table 3). The apparent ϕ of CMs in control sample was 0.118, which agreed with values reported

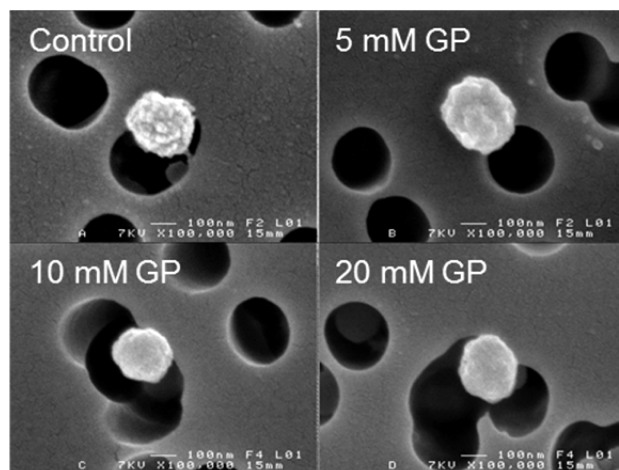


Figure 3. Representative pictures obtained by scanning electron microscopy of CMs present in the control sample and in samples containing 5, 10, and 20 mM GP. The magnification was $\times 100\,000$.

in the literature³⁴ for suspensions of CMs at 25 g L^{-1} (Table 3). In the GP added samples, the apparent ϕ of CMs were gradually reduced until reaching 0.0689 in the presence of 20 mM GP. ϕ of CMs calculated from average D_h (Table 3) also decreased according to the GP addition.

The values of γ are presented as a function of time in Figure 4. Note first that γ was strongly reduced in all the samples within the first second, i.e., on shorter times than the apparatus resolution. The first measurement of γ is in fact made 1–2 s after the drop formation, and during this time γ has already decreased from the value of a bare interface ($\sim 72\text{ mN m}^{-1}$ at $20\text{ }^\circ\text{C}$) corresponding to pure water to values of the order of $45\text{--}50\text{ mN m}^{-1}$. This strong and fast dynamics was then not accessible with this apparatus. However, following the first sharp decay of γ , a slower dynamics of adsorption at the air/water interfaces was then observed, and a plateau value was eventually reached. This second stage as well as the final γ was different between the suspensions. For the control and sample containing 5 mM GP, the first fast decay of the surface tension almost leads to the final equilibrium value, and only a slight reduction of γ is measured before reaching the equilibrium at values of 45.7 ± 0.1 and $47.4 \pm 0.1\text{ mN m}^{-1}$, respectively. Thus,

Table 2. Average Hydrodynamic Diameters (D_h) and Zeta Potentials of CMs Containing Different GP Concentrations^a

	control sample	5 mM GP	10 mM GP	20 mM GP
average D_h (nm)				
in HEPES buffer	179 ± 5	164 ± 3	163 ± 4	160 ± 2
in 100 mM citrate	*	189 ± 3	184 ± 3	177 ± 3
in 8 M urea	*	184 ± 4	175 ± 3	173 ± 3
zeta potential ζ (mV)	-18.4 ± 2.7	-21.5 ± 2.3	-23.4 ± 2.8	-26.0 ± 3.1

^a D_h of CMs were determined in HEPES buffer, or 100 mM citrate (as Ca-chelating agent), or 8 M urea (as denaturing agent). The * symbol indicates that determination of D_h by DLS was impossible.

Table 3. η and φ , E^* , E' , and E'' of CMs Suspensions Containing Different GP Concentrations

	control	5 mM GP	10 mM GP	20 mM GP
η (mPa s ⁻¹)	1.655 ± 0.063	1.581 ± 0.043	1.483 ± 0.014	1.441 ± 0.020
apparent φ	0.118	0.102	0.080	0.069
φ from D_h	0.103	0.079	0.077	0.073
E^* (mN m ⁻¹)	23.2 ± 1.2	14.0 ± 0.6	12.0 ± 0.3	15.4 ± 1.0
E'' (mN m ⁻¹)	12.2 ± 0.5	7.9 ± 0.5	4.5 ± 0.2	2.2 ± 0.1
E' (mN m ⁻¹)	19.7 ± 1.2	11.5 ± 0.5	11.1 ± 0.2	15.2 ± 1.0

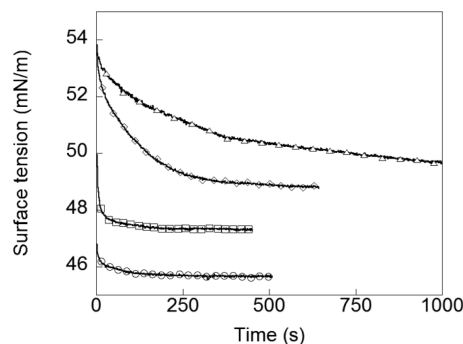


Figure 4. Surface tension (γ) as a function of time at air/water interface of control sample (\circ) and samples containing 5 (\square), 10 (\diamond), and 20 (\triangle). For clarity, not all data points are indicated by symbols.

qualitatively, these two samples have a similar behavior. Oppositely, in the presence of 10 and 20 mM GP, the samples needed considerably higher times to attain the plateau, located respectively at 48.8 ± 0.3 and 49.6 ± 0.7 mN m⁻¹. Note that there are still a first fast decay of γ (in less than 1 s), but this is followed by a second regime, with a typical time scales of hundred of seconds.

The interfacial complex modulus E^* and its elastic (E') and viscous (E'') contributions are given in Table 3. The control sample presented the highest E^* , the sample containing 20 mM GP an intermediate value, and those containing 5 and 10 mM GP showed similar and the lowest values. More pronounced was the vanishing of the viscous modulus E'' as GP was added. As shown in Figure 5, there was no phase shift between surface tension and drop volume at 20 mM GP, while there was a shift of 32° for the control sample. As a consequence, E' was almost similar to E'' for the control sample (i.e., viscoelastic behavior of the interfacial layer), while $E' \gg E''$ for large amount of GP (i.e., solid-like behavior of the adsorbed layer).

DISCUSSION

In this section, the results are grouped and rationalized following ascending length scales. From a molecular level, we demonstrate that caseins were cross-linked by GP at lysyl and arginyl residues forming a covalent bound matrix. Next, from the particle-scale data, we confirm that the cross-linking reaction modified the CMs (e.g., decrease of size and charge, surface smoothing). From a combined particle-bulk scale, we deduce the intramolecular nature of the GP cross-linking (by the reduction in viscosity), and we discuss how cross-linked CMs behave in the presence of dissociating agents (citrate and urea) and under interfacial stress using a highly hydrophobic wall (air–water interface).

Characterization of the Reaction between CMs and GP. When GP was added to CM suspensions, blue pigments absorbing at 607 nm were formed.²³ The development of this

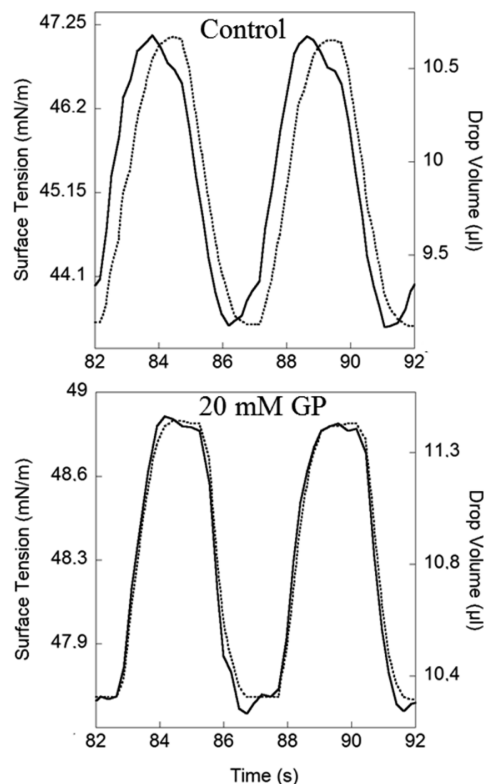


Figure 5. Shifts in phase angle between drop volume oscillation and the changes in γ at a frequency of 0.2 Hz of control sample and sample containing 20 mM GP. The solid line corresponds to γ and the dotted line to drop volume.

blue color as a function of GP concentration proved that caseins reacted with GP (Figure 1). The maximum of absorption of the reacted products at 607 nm and the fact that the reaction was more intense when the GP concentration increased were in accordance with the literature.^{35,36} In our case, the mechanism of the reaction was not determined, but it is accepted that the reaction progress in two stages. In a first time, GP forms a monomeric adduct, and then it cross-links the protein units.³⁷

The total amino acids analysis showed that lysyl and arginyl residues were involved in the reaction (Table 1), certainly because these two amino acids have with free NH₂ groups. However, they were consumed at different levels (Lys > Arg). This difference of reactivity could be due to different ionization states at the pH of the suspensions. The pK_a values of the NH₂ group of lysyl and arginyl residues are 10.5 and 12.5, respectively. At pH 7.10, the ratio [NH₃⁺/NH₂] for Arg is 100 times higher than for Lys. It was shown that the level of reacted NH₂ can be doubled by changing the pH from 6.75 to 10.5 (depending on the molar proportions).³⁵ It highlights the effect of reducing the ratio [NH₃⁺/NH₂] in the efficiency of the

reaction. Generally, the consumption of free NH_2 is below 85% with respect to the total available NH_2 , even in excess of GP.^{35,36} The reasons are based on factors like pH, temperature, molar proportion, accessibility of NH_2 groups (which depends on protein type and structure), and also some degree of reversibility of the reaction. These elements could explain the presence of unreacted GP when 10 and 20 mM GP were added to CMs suspensions (Table 1). In addition, it was shown by mass spectrometry that GP can self-polymerize to form molecular associations containing 10–26 GP molecules.³⁵

By RP-HPLC, it was possible to separate casein molecules according to their hydrophobicity after submitting the CMs to dissociation conditions. For control sample, the elution profile of the caseins molecules was in accordance with the literature³² (Figure 2). In sample containing 5 mM GP, only traces of individual caseins were found (Figure 2). This underlined that even consuming 3.87 mM of NH_2 from the total 20.1 mM available (Table 1), most of the casein molecules were covalently trapped within the protein matrix. In the presence of 10 and 20 mM GP, no individual casein molecules were observed. The chromatographic peak at the end of the elution (Figure 2) was not resolved by RP-HPLC. An additional experiment by electrophoresis (SDS-PAGE) revealed that the compounds formed between casein molecules and GP were unable to migrate through a gel made with 10% of polyacrylamide (data not shown).

These results and the set of the following arguments suggested that the products of the reaction were essentially composed of cross-linked CMs. Indeed, casein molecules are unfolded (rheomorphic³) proteins which possess a high number of free NH_2 groups (at least 9 lysine and 4 arginine per molecule²). They are highly concentrated within the CMs: one average CM contains $\sim 5 \times 10^3$ casein molecules present in a volume of about $2.1 \times 10^{-3} \mu\text{m}^3$.³⁸ The CMs are porous structures, and GP is a small molecule with a low molecular weight (226 g mol^{-1}); thus, it could easily move through the protein matrix. In addition, we showed that only traces of individual caseins were observed when 5 mM GP was added (Table 1 and Figure 2). In practice, there was high probability that all casein molecules were cross-linked within the CMs. Nevertheless, we must admit that we have only a global view of the reaction between GP and caseins.

Modification of CMs by GP: Compiling Data at the Particle Scale. Concerning the average D_h of CMs, a slight but significant decrease was observed by DLS (Table 2) after reaction with GP. Justifying this decrease in D_h by shrinkage of CMs upon GP cross-linking remains uncertain because we did not study their internal structure. Notwithstanding, the height of the hairy layer of κ -casein was previously calculated as $\sim 12 \text{ nm}$.³⁹ Hence, an anchorage of the hairy layer onto the surface of the micelle is plausible. This argument was strengthened by the SEM observation of particles (Figure 3). The SEM images highlighted a clear smoothing on the surface of CMs as a function of GP concentration, suggesting that their external parts were affected by the reaction. The decrease of ζ , according to the GP addition, was also consistent with these observations. Indeed, κ -caseins, located on the surface of CMs,⁴⁰ are the main responsible for their negative charge.¹ This casein molecule possesses 9 lysyl and 5 arginyl residues² that are potentially available for cross-linking. At pH 7.10, the ratios $[\text{NH}_3^+/\text{NH}_2]$ are 2.2×10^3 and 2.2×10^5 for lysyl and arginyl residues, respectively. We presume that insofar as NH_2 was consumed in the reaction, the ratio $[\text{NH}_3^+/\text{NH}_2]$ was re-

established; consequently, the positive contribution of NH_3^+ for the net charge decreased, and the particles became more negatively charged.

An Intracellular Nature of the Cross-Linking Reaction. In fact, it is interesting to note that no aggregated particles were observed by DLS. Considering that the intensity of the scattered light scale like to δ^6 (where δ is a particle size), aggregated CMs should be easily seen by this technique. These results indicate that cross-linking reaction was intracellular. The following discussion about η and φ conduces to the same inference.

Regarding η , all samples behaved as Newtonian fluids (Table 3), which is expected for suspensions of CMs below 100 g L^{-1} interacting only through excluded volume effects.²⁸ The apparent φ of CMs, calculated from η , decreased as a function of GP concentration (Table 3). φ depends on the third power of the particle radius. Then, keeping constant other parameters, the reduction of apparent φ underlined a reduction of the hydrodynamic size of particles and the absence of aggregates.

The intracellular nature of the cross-linking could be somewhat expected due to electrostatic and steric repulsions between CMs.⁷ Indeed, CMs only start to form “dumbbells” (pair of CMs moving together) at φ values greater than 0.15.⁴¹ When the average D_h was used to calculate φ of CMs (Table 3), a gradual reduction of φ was also observed, but the magnitude of the reduction was different between the two methods. The objective of using viscosity and DLS was to provide evidence that the average size of CMs was reduced upon genipin cross-linking and also that the reaction was intracellular. Keeping the micellar unit was of central importance for our work. Therefore, the comparison of the results from viscosity and DLS showed the self-consistency of our findings by verifying a same tendency on the data. When different techniques are applied to calculate φ , inaccuracy and systematic errors are unavoidable.⁴²

Stability of CMs in the Presence of Dissociating Agents. The stability of CMs in the presence of dissociating agents was evaluated by DLS after the dilution of samples in 100 mM sodium citrate or 8 M urea (Table 2). It is known that sodium citrate induces the solubilization of CCP and causes dissociation of CMs.¹³ In the control sample, the CMs were dissociated and not observed by DLS. On the contrary, in the GP added samples, the CMs did not dissociate and swelled inversely to GP concentration. A similar effect was observed in CMs cross-linked by transglutaminase in the presence of 50 mM sodium citrate.¹⁶ In fact, when the CCP is solubilized at neutral pH, the negative charges of the phosphate centers of α_{S1} -, α_{S2} -, and β -casein are exposed. As a consequence, the cross-linked CMs swollen due to the electrostatic repulsions generated in the core of the particles, and the increase in the hydration of the uncovered protein sequences containing the phosphate centers. The more the CMs were cross-linked, the higher were their resistances to swelling.

Urea makes strong H-bonds with water and causes disruption of hydrophobic and hydrophilic interactions of proteins.⁴³ When urea is added to a suspension of CMs ($>6 \text{ M}$ urea), CMs dissociate as a result of the rupture of hydrophobic interactions between the tails of caseins that are surrounding the nanoclusters of CCP.^{3,44} Our results showed that, in the presence of 8 M urea, the control CMs (control sample) dissociated and were not observed by DLS, whereas in the samples containing GP, CMs resisted to the dissociation and swelled inversely to GP concentration (Table 2). Comparable

results were observed for CMs cross-linked by transglutaminase in the presence of 6 M urea.^{6,16} Two different explanations for this phenomenon were raised by the authors. In a first work,¹⁶ the authors interpreted the swelling as a consequence of a “hydrophobic hydration” of the polymer chains within the CMs. In a second work,⁶ the authors did not observe significant differences between the SANS spectra of control and cross-linked CMs, and attributed the increase in D_h to the presence of “dangling” ends formed after the disruption of weak interactions by urea. Our results showed that the resistance to swelling was proportional to the intensity of the cross-linking. Hence, if the formation of “dangling ends” is true, it must be inversely correlated to GP cross-linking.

The colloidal properties of CMs were progressively changed by the GP cross-linking, whereas the micellar unit was preserved. The cross-linked CMs swelled after solubilization of CCP by 100 mM sodium citrate or in the presence of 8 M urea. This behavior is typical of hydrogels,⁴⁵ and henceforward, the cross-linked CMs are referred as casein microgels due to their dimensions.

Stability of CMs at the Air/Water Interface. Caseins are surface-active proteins and even at low concentrations adsorb at air/water interfaces, hence reducing γ .⁴⁶ Indeed, the air–water interface is the most hydrophobic surface possible. Interfacial adsorption is then sufficient to modify a polymer or a protein configuration in order to expose the hydrophobic moieties to air. Not only the configurations of single molecules are modified once adsorbed, bulk micelles are also generally disintegrated at air–solution interfaces. In that respect, investigating interfacial properties provides information on how supramolecular structures resist to the presence of a highly hydrophobic wall.

The decrease of γ as a function of time for the control sample (Figure 4) was similar to those found for skim milk.⁴⁷ The initial reduction of γ (within the first second) implies adsorption of large amount of matter at the air/water interface. This dynamics was fast (less than 1 s) but was fully consistent with the large value of the casein concentration ($c = 25 \text{ g L}^{-1}$). The full dynamics of γ was then attributed to dissociation of CMs as they approach the interface, to casein monomer adsorption, and to reorganization of these entangled casein monomers at the interface. This argument is consistent with the fact that a previous dissociation of CMs with EDTA⁴⁷ can lead to even faster dynamics. The sample containing 5 mM GP presented a similar behavior to the control sample; i.e., the fast dynamical process almost leads to the final value. However, the equilibrium value is higher than for the control sample (Figure 4), probably as the effect of CM cross-linking start to be detected.

As described previously, the dynamics of adsorption for the suspensions containing 10 and 20 mM GP turns out to be significantly different. Two consecutive processes were detected, but with very different time scales: even if the first and rapid decay was still observed, it was much less efficient to cover the interface on short times (i.e., to reduce the surface tension), and it was then followed by a second slow process, finally providing less interfacial coverage (higher γ at equilibrium on Figure 4 for high GP concentrations). In these samples, we believe that this slow second stage was linked to the adsorption of only the casein microgels, while keeping their supramolecular integrity. This explains the slower dynamics (large colloidal objects diffuse toward the interface slower than single proteins, and the adsorption mechanism is

also slower) and the less efficient interfacial coverage (colloids cannot pack on a 2D interface as well as single proteins adsorbing at a molecular scale). In the casein microgels, the protein matrices are indeed sufficiently cross-linked to resist to the usual destruction of their supramolecular structure. As consequence, no other free casein molecules are delivered to rapidly and further cover the interface as in the control sample. Note also that, at the highest GP concentration, a true equilibrium value is not measured. Such a slow and never-ending decrease in γ can then be related to a reorganization of the casein microgels themselves at the interface, similar to a glassy evolution. Similar behaviors were observed for aggregates of β -lactoglobulin, with sizes ranging from 30 to 117 nm.⁴⁸ As the surface tension dynamics is complex (with different fast and slow processes, presence of micelles), it is not relevant to try to fit such data with simple models. A complete analysis of these data is beyond the scope of this article. Here direct comparisons already allowed us to evidence the strong stability of the casein microgels. Moreover, these different types of interfacial structure were also confirmed by the interfacial rheological studies.

A viscoelastic interface was observed for the control sample (Table 3 and Figure 5), which presented the highest E^* and a significant contribution of E'' . A significant viscous contribution E'' is related to relaxation mechanisms and rearrangement within the adsorbed layer.⁴⁹ This implies that once the CMs lost their structure, the casein molecules can interact and form a gelified viscoelastic layer, made of entangled casein chains.

By contrast, the results for the suspensions containing high contents of GP were more unusual. The facts that E'' was vanished (Table 3) and θ shifted toward 0° (Figure 5) as GP was added rule out the presence of an interfacial gel made of casein chains and mean that the interfacial layer has the mechanical properties of a solid plate. This type of response corresponds to the one of a monolayer of nonpenetrable and repulsive particles, thus having no possible dissipation or relaxation processes. All together, these interfacial results are consistent with the fact that, with GP, the CMs can be considered as highly stable and internally cross-linked microgels. Such particles were still able to adsorb at the air–solution interface and to significantly decrease γ . Furthermore, the casein microgels resisted to the dissociating effect of a hydrophobic wall as well as to interfacial compression stresses.

CONCLUSION

GP reacted with caseins molecules forming blue pigments that absorb at 607 nm. The reaction concerned lysyl and arginyl residues. The greater reactivity of lysyl residues was attributed to its lower pK_a . No individual caseins were observed when 10 and 20 mM GP were added, suggesting that all casein molecules formed a covalently linked protein matrix. The cross-linking reaction induced changes on the colloidal properties of the particles. The decrease in size of casein microgels with respect to control CMs was accounted for the involvement of free NH_2 of the external layer of κ -casein. The gradual smoothing of their surfaces and the reduction of ζ corroborated with this hypothesis. The DLS and rheological measurements indicated that the cross-linking was intramicellar, once one single population was observed and the values of η (and consequently φ) were gradually reduced. The casein microgels swelled but were resistant to dissociation in the presence of 100 mM sodium citrate or 8 M urea. Contrarily, to control CMs, such microgels did not dissociate under interfacial

adsorption and compression stresses and formed rigid interfacial layers.

Further studies are needed to apprehend the main factors involved in the reaction of caseins with GP. These studies should be done with isolated casein molecules. Additionally, it could be interesting to investigate the consequences of the cross-linking on the internal structure of casein microgels as well as to understand their colloidal behavior in different physicochemical conditions (temperature, pH, ionic strength, presence of divalent cations, organic solvents, etc.).

Among the perspectives of this work, the use of casein microgels as adaptable nanocarriers is envisaged. Recent studies have shown that CMs can be used as a vehicle for hydrophobic molecules.^{50–52} Taking into account the sensitivity of the structure of control CMs face to the ionic environment,³ the casein microgels can potentially replace CMs in this purpose. In addition, the minerals (CCP) can be removed from the casein microgels (e.g., by adding sodium citrate) without destroying their structure. Then, thousands of negatively charged groups (pH-dependent) are generated in the core of the particles. In addition to these groups, there are already thousands of partially dissociated carboxylic groups as follows from the amino acid composition, pK_a , and number and proportion of casein molecules. Hence, the casein microgels can be potentially used for an intelligent pH-triggered capture/release of charged nutraceutical molecules.

AUTHOR INFORMATION

Corresponding Authors

*E-mail: nogueira@rennes.inra.fr (N.F.N.S.).

*E-mail: frederic.gaucheron@rennes.inra.fr (F.G.).

Notes

The authors declare no competing financial interest.

ACKNOWLEDGMENTS

The authors acknowledge the financial support from Région Bretagne, under grant ARED 6188. The authors thank Michel Piot for his precious help with the physicochemical analyses.

REFERENCES

- Dalgleish, D. G. On the structural models of bovine casein micelles—review and possible improvements. *Soft Matter* **2011**, *7* (6), 2265–2272.
- Swaisgood, H. E. Chemistry of Caseins. In *Advanced Dairy Chemistry - Proteins Part A*, 3rd ed.; Fox, P. F., McSweeney, P. L. H., Eds.; Kluwer Academic/Plenum Publishers: New York, 2003; Vol. 1, pp 139–201.
- de Kruijff, C. G.; Holt, C. Casein Micelle Structure Functions and Interactions 1. In *Advanced Dairy Chemistry - Proteins Part A*, 3rd ed.; Fox, P. F., McSweeney, P. L. H., Eds.; Kluwer Academic/Plenum Publishers: New York, 2003; Vol. 1, pp 233–276.
- Walstra, P.; Wouters, J. T. M.; Geurts, T. *Dairy Science and Technology*, 2nd ed.; Taylor & Francis Group: Boca Raton, FL, 2006; Vol. 3, pp 109–157.
- Holt, C.; Timmins, P. A.; Errington, N.; Leaver, J. A core-shell model of calcium phosphate nanoclusters stabilized by beta-casein phosphopeptides, derived from sedimentation equilibrium and small-angle X-ray and neutron-scattering measurements. *Eur. J. Biochem.* **1998**, *252* (1), 73–78.
- de Kruijff, C. G.; Huppertz, T.; Urban, V. S.; Petukhov, A. V. Casein micelles and their internal structure. *Adv. Colloid Interface Sci.* **2012**, *171*, 36–52.
- Tuinier, R.; de Kruijff, C. G. Stability of casein micelles in milk. *J. Chem. Phys.* **2002**, *117* (3), 1290–1295.
- Trejo, R.; Dokland, T.; Jurat-Fuentes, J.; Harte, F. Cryo-transmission electron tomography of native casein micelles from bovine milk. *J. Dairy Sci.* **2011**, *94* (12), 5770–5775.
- Holt, C.; Horne, D. S. The hairy casein micelle: Evolution of the concept and its implications for dairy technology. *Neth. Milk Dairy J.* **1996**, *50* (2), 85–111.
- McGann, T. C. A.; Fox, P. F. Physico-chemical properties of casein micelles reformed from urea-treated milk. *J. Dairy Res.* **1974**, *41* (01), 45–53.
- Vaia, B.; Smiddy, M. A.; Kelly, A. L.; Huppertz, T. Solvent-mediated disruption of bovine casein micelles at alkaline pH. *J. Agric. Food Chem.* **2006**, *54* (21), 8288–8293.
- Lin, S. H. C.; Leong, S. L.; Dewan, R. K.; Bloomfield, V. A.; Morr, C. V. Effect of calcium ion on the structure of native bovine casein micelles. *Biochemistry* **1972**, *11* (10), 1818–1821.
- Pitkowski, A.; Nicolai, T.; Durand, D. Scattering and turbidity study of the dissociation of casein by calcium chelation. *Biomacromolecules* **2008**, *9* (1), 369–375.
- Dalgleish, D. G.; Corredig, M. The Structure of the Casein Micelle of Milk and Its Changes During Processing. *Annu. Rev. Food Sci. Technol.* **2012**, *3*, 449–467.
- Audic, J. L.; Chaufer, B.; Daufin, G. Non-food applications of milk components and dairy co-products: A review. *Lait* **2003**, *83* (6), 417–438.
- Huppertz, T.; Smiddy, M. A.; de Kruijff, C. G. Biocompatible micro-gel particles from cross-linked casein micelles. *Biomacromolecules* **2007**, *8* (4), 1300–1305.
- Huppertz, T.; de Kruijff, C. G. Structure and stability of nanogel particles prepared by internal cross-linking of casein micelles. *Int. Dairy J.* **2008**, *18* (5), 556–565.
- Song, F.; Zhang, L. M.; Yang, C.; Yan, L. Genipin-crosslinked casein hydrogels for controlled drug delivery. *Int. J. Pharm.* **2009**, *373* (1–2), 41–47.
- Endo, T. O. H. R.; Taguchi, H. E. I. H. The Constituents of Gardenia jasminoides geniposide and genipin-gentiobioside. *Chem. Pharm. Bull.* **1973**, *21* (12), 2684–2688.
- Sung, H. W.; Huang, R. N.; Huang, L. L. H.; Tsai, C. C. In vitro evaluation of cytotoxicity of a naturally occurring cross-linking reagent for biological tissue fixation. *J. Biomater. Sci., Polym. Ed.* **1999**, *10* (1), 63–78.
- Pierre, A.; Fauquant, J.; Le Graet, Y.; Piot, M.; Maubois, J. L. Préparation de phosphocaseinate natif par microfiltration sur membrane. *Lait* **1992**, *72* (5), 461–474.
- Schuck, P.; Piot, M.; Mejean, S.; Le Graet, Y.; Fauquant, J.; Brulé, G.; Maubois, J. L. Déshydratation par atomisation de phosphocaseinate natif obtenu par microfiltration sur membrane. *Lait* **1994**, *74* (5), 375–388.
- Lee, S. W.; Lim, J. M.; Bhoo, S. H.; Paik, Y. S.; Hahn, T. R. Colorimetric determination of amino acids using genipin from Gardenia jasminoides. *Anal. Chim. Acta* **2003**, *480* (2), 267–274.
- Davies, M. G.; Thomas, A. J. An investigation of hydrolytic techniques for the amino acid analysis of foodstuffs. *J. Sci. Food Agric.* **1973**, *24* (12), 1525–1540.
- Spackman, D. H.; Stein, W. H.; Moore, S. Automatic recording apparatus for use in chromatography of amino acids. *Anal. Chem.* **1958**, *30* (7), 1190–1206.
- Sheu, S. J.; Hsin, W. C. HPLC separation of the major constituents of Gardenia fructus. *J. High Resolut. Chromatogr.* **1998**, *21* (9), 523–526.
- Silva, N. N.; Piot, M.; de Carvalho, A. F.; Violleau, F.; Fameau, A. L.; Gaucheron, F. pH-induced demineralization of casein micelles modifies their physico-chemical and foaming properties. *Food Hydrocolloids* **2013**, *32* (2), 322–330.
- Bouchoux, A.; Debbou, B.; Gesan-Guiziu, G.; Famelart, M. H.; Doublier, J. L.; Cabane, B. Rheology and phase behavior of dense casein micelle dispersions. *J. Chem. Phys.* **2009**, *131* (16), 165106–165111.
- Glantz, M.; Hakansson, A.; Mansson, H. L.; Paulsson, M.; Nilsson, L. Revealing the size, conformation, and shape of casein

micelles and aggregates with asymmetrical flow field-flow fractionation and multiangle light scattering. *Langmuir* **2010**, *26* (15), 12585–12591.

(30) Ravera, F.; Loglio, G.; Kovalchuk, V. I. Interfacial dilational rheology by oscillating bubble/drop methods. *Curr. Opin. Colloid Interface Sci.* **2010**, *15* (4), 217–228.

(31) Benjamins, J.; Cagna, A.; LucassenReynders, E. H. Viscoelastic properties of triacylglycerol/water interfaces covered by proteins. *Colloids Surf., A* **1996**, *114*, 245–254.

(32) Leonil, J.; Molle, D.; Gaucheron, F.; Arpino, P.; Guenot, P.; Maubois, J. L. Analysis of major bovine-milk proteins by online high-performance liquid-chromatography and electrospray-ionization mass-spectrometry. *Lait* **1995**, *75* (3), 193–210.

(33) Dagleish, D. G.; Spagnuolo, P. A.; Goff, H. D. A possible structure of the casein micelle based on high-resolution field-emission scanning electron microscopy. *Int. Dairy J.* **2004**, *14* (12), 1025–1031.

(34) de Kort, E.; Minor, M.; Snoeren, T.; van Hooijdonk, T.; van der Linden, E. Effect of calcium chelators on physical changes in casein micelles in concentrated micellar casein solutions. *Int. Dairy J.* **2011**, *21* (12), 907–913.

(35) Qi, P. X.; Nunez, A.; Wickham, E. D. Reactions between beta-lactoglobulin and genipin: Kinetics and characterization of the products. *J. Agric. Food Chem.* **2012**, *60* (17), 4327–4335.

(36) Yao, C. H.; Liu, B. S.; Chang, C. J.; Hsu, S. H.; Chen, Y. S. Preparation of networks of gelatin and genipin as degradable biomaterials. *Mater. Chem. Phys.* **2004**, *83*, 204–208.

(37) Fujikawa, S.; Nakamura, S.; Koga, K.; Genipin, A. New type of protein crosslinking reagent from gardenia fruits. *Agric. Biol. Chem.* **1988**, *52* (3), 869–870.

(38) Fox, P. F.; Brodtkorb, A. The casein micelle: Historical aspects, current concepts and significance. *Int. Dairy J.* **2008**, *18* (7), 677–684.

(39) Holt, C.; Dagleish, D. G. Electrophoretic and hydrodynamic properties of bovine casein micelles interpreted in terms of particles with an outer hairy layer. *J. Colloid Interface Sci.* **1986**, *114* (2), 513–524.

(40) Dagleish, D. G.; Horne, D. S.; Law, A. J. R. Size-related differences in bovine casein micelles. *Biochim. Biophys. Acta* **1989**, *991* (3), 383–387.

(41) Nobel, S.; Weidendorfer, K.; Hinrichs, J. Apparent voluminosity of casein micelles determined by rheometry. *J. Colloid Interface Sci.* **2012**, *386*, 174–180.

(42) Poon, W. C. K.; Weeks, E. R.; Royall, C. P. On measuring colloidal volume fractions. *Soft Matter* **2012**, *8* (1), 21–30.

(43) Walstra, P. *Physical Chemistry of Foods*; Marcel Dekker Inc.: New York, 2002.

(44) Holt, C. Casein micelle substructure and calcium phosphate interactions studied by sephacryl column chromatography. *J. Dairy Sci.* **1998**, *81* (11), 2994–3003.

(45) Nayak, S.; Lyon, L. A. Soft nanotechnology with soft nanoparticles. *Angew. Chem., Int. Ed.* **2005**, *44* (47), 7686–7708.

(46) Leman, J.; Kinsella, J. E. Surface-activity, film formation, and emulsifying properties of milk-proteins. *Crit. Rev. Food Sci. Nutr.* **1989**, *28* (2), 115–138.

(47) Cases, E.; Rampini, C.; Cayot, P. Interfacial properties of acidified skim milk. *J. Colloid Interface Sci.* **2005**, *282* (1), 133–141.

(48) Rullier, B.; Novales, B.; Axelos, M. A. V. Effect of protein aggregates on foaming properties of beta-lactoglobulin. *Colloids Surf., A* **2008**, *330* (2-3), 96–102.

(49) Williams, A.; Prins, A. Comparison of the dilational behaviour of adsorbed milk proteins at the air-water and oil-water interfaces. *Colloids Surf., A* **1996**, *114*, 267–275.

(50) Haham, M.; Ish-Shalom, S.; Nodelman, M.; Duek, I.; Segal, E.; Kustanovich, M.; Livney, Y. D. Stability and bioavailability of vitamin D nanoencapsulated in casein micelles. *Food Funct.* **2012**, *3* (7), 737–744.

(51) Livney, Y. D. Milk proteins as vehicles for bioactives. *Curr. Opin. Colloid Interface Sci.* **2010**, *15* (1-2), 73–83.

(52) Sahu, A.; Kasoju, N.; Bora, U. Fluorescence study of the curcumin-casein micelle complexation and its application as a drug

nanocarrier to cancer cells. *Biomacromolecules* **2008**, *9* (10), 2905–2912.